Accurate Determination of the Equilibrium and Vibrationally Averaged Structural and Molecular Properties of Difluoromethanimine (F_2CNH) from ab Initio Calculations

Cristina Puzzarini*,† and Alberto Gambi‡

Dipartimento di Chimica "G. Ciamician", Università di Bologna, Via Selmi 2, I-40126 Bologna, Italy, and Dipartimento di Scienze e Tecnologie Chimiche, Università di Udine, Via Cotonificio 108, I-33100 Udine, Italy

Received: January 13, 2004; In Final Form: March 2, 2004

The availability of large core-valence basis sets together with highly accurate coupled-cluster calculations allow us to present an improved determination of the equilibrium structure of the difluoromethanimine molecule. Core correlation effects and basis set incompleteness have been taken into account to obtain best estimates of the equilibrium geometry. In addition, two important molecular properties, namely, the dipole moment and the nuclear quadrupole coupling constants, have been investigated. The molecular dipole moment has been calculated at the coupled-cluster level using basis sets of different quality, including diffuse functions and taking into account both core correlation effects and basis set incompleteness. The quadrupole coupling constants, evaluated from the electric field gradient at the quadrupolar nuclei, have been computed at the multiconfiguration self-consistent field, Møller−Plesset perturbation to second order, and coupled-cluster levels of theory employing large core-valence basis sets. Because experiment usually determines vibrational ground state molecular parameters, to directly compare theoretical and experimental results a vibrational averaging procedure has been carried out. This allowed us to evaluate the vibrational corrections both for the molecular structure and properties investigated.

1. Introduction

The first investigations on difluoromethanimine, F_2CNH, were carried out in 1988.[1] In that year, for the first time Bürger and Pawelke prepared, isolated, and characterized the molecule and assigned its vibrational spectrum. Despite its instability, F_2CNH could be maintained for a long time in the gaseous phase at relatively low values of pressure. This allowed in the same year the investigation of the microwave spectra with the determination of the ground-state rotational constants and molecular properties, such as the dipole moment and nuclear quadrupole coupling constants.[2,3]

Subsequently, in 1992 Bürger et al.[4] recorded the high-resolution FTIR spectra of F_2CNH in the mid-infrared region. This experimental investigation was accompanied by ab initio calculation of the harmonic and anharmonic force field. In the same year, Pawelke et al.[5] carried out the characterization of F_2CNH by NMR, infrared and photoelectron spectroscopy; in addition, they determined the structure of this molecule by single-crystal X-ray diffraction, putting in evidence the planarity of the molecule.

A few years later, in 1996, Groner and co-workers observed the microwave spectra of the ^{13}C-, ^{15}N- and ^{15}N,D-substituted species. From the ground-state rotational constants of these four isotopomers, the first evaluation of the r_0 structure was performed.[6]

More recently, Groner and Warren presented the determination of approximate r_e structures from experimental rotational constants and an ab initio force field for a few molecules including F_2CNH.

In 2002, two theoretical works were published, both of them regarded the computation of the anharmonic force field of difluoromethanimine. One of the authors carried out an improved determination of the anharmonic force field at the CCSD(T)-MP2 level of theory,[8] whereas Pouchan and Gelize-Duvignau evaluated the quartic force field at the CI level.[9]

The experimental data determined so far, as well as the highly accurate ab initio methods and the large and property-oriented basis sets available, stimulated the present investigation. In particular, we would like to clarify some controversial experimental results, such as those for the molecular dipole moment. To properly compare theoretical and experimental data, a vibrational averaging procedure for evaluating the zero-point vibrational corrections has also been performed.

2. Computational Details

Geometry optimizations and dipole moment evaluations have been carried out by employing the CCSD(T) method,[10−12] where the acronym stands for coupled-cluster with all single and double excitations (CCSD) augmented by a quasiperturbative account for triples substitutions (T). A few geometry optimizations have also been performed using Møller−Plesset perturbation theory to second order[13] (MP2). In general, the frozen core approximation has been adopted in the computations; i.e., only valence electrons have been correlated. Only in the case of core-valence basis sets, all electrons correlated calculations have also been carried out. More precisely, for geometry optimizations the correlation consistent valence cc-pV*n*Z (n = Q, 5)[14] and the weighted core-valence cc-pwCV*n*Z (n = T, Q, 5)[14,15] bases have been used. As regards the molecular dipole moment, because inclusion of diffuse functions in the basis set is particularly important for an accurate evaluation of this property, the aug-cc-pV*n*Z (n = T, Q, 5)[14,16,17] and the aug-cc-pwCV*n*Z (n = T, Q) basis sets have been employed. The aug-cc-pwCV*n*Z sets have been obtained by adding the diffuse functions of the aug-cc-pV*n*Z bases[14,16] to the cc-pwCV*n*Z sets.

* Corresponding author. E-mail: criss@ciam.unibo.it.
† Università di Bologna.
‡ Università di Udine.

10.1021/jp049838p CCC: $27.50
Published on Web 04/14/2004

It is worth noting that in geometry optimizations we have used the weighted core-valence cc-pwCV*n*Z bases instead of the traditional cc-pCV*n*Z sets[18] because it is well proved that they significantly improve the convergence of many molecular properties with *n*.[15] This is also confirmed by some of our test computations: even for difluoromethanimine, which contains only first-row atoms, for a given value of *n* the cc-pwCV*n*Z bases give distances shorter by about 0.0005−0.001 Å (depending on the bond type and *n*) than those obtained with the cc-pCV*n*Z sets (all electrons correlated). On the other hand, bond angles do not seem to be affected. As concerns dipole moment evaluations, very small variations have been found, i.e., of the order of 0.001 D, when the aug-cc-pwCV*n*Z sets are used instead of the aug-cc-pCV*n*Z ones.

As far as all electron computations are concerned, because all electron CCSD(T)/cc-pwCV5Z calculations require a very large computational effort and, as demonstrated by Demaison and co-workers,[19−21] the MP2 method can be sufficient to estimate core correlation corrections, the geometry optimizations employing the cc-pwCV5Z basis set have been carried out at the MP2 level.

The elements of the inertial nuclear quadrupole coupling tensors of nitrogen and deuterium nuclei have been determined from electric field gradient calculations carried out using the multiconfiguration self-consistent field (MCSCF),[22,23] MP2[13,24] and CCSD[24,25] methods. As concerns the MCSCF approach, we have performed complete active space self-consistent field (CASSCF) computations with 20 valence electrons in 15 orbitals as an active space; this corresponds to the full valence minus the 2s orbitals on the F atoms. This active space has been chosen after some test computations that were carried out employing a basis of triple-ζ quality and different active spaces: orbital character, energies, and occupations have been carefully checked and results compared. In particular, it has been checked that the 2s fluorine orbitals, excluded from the active space, do not present any considerable mixing with the 2p fluorine orbitals. It has been found that the CAS space chosen is able not only to provide results in very good agreement with those obtained with all the valence shell taken as active (24 electrons in 17 orbitals) but also to allow calculations with very large quadruple and quintuple ζ basis sets (nearly impossible computations with all valence electrons as active). In regard to the MP2 and CCSD calculations, all electrons have been correlated. Because an accurate description of the inner valence and core regions is needed for electric field gradient evaluations, as highlighted by Halkier and co-workers,[24,26] the cc-pwCV*n*Z (n = T, Q, 5) basis sets have been employed in these calculations.

The MOLPRO ab initio package[10,27−29] and the DALTON program[30] have been used throughout. More precisely, MOLPRO has been employed in geometry optimizations, dipole moment, and electric field gradient evaluations, whereas the DALTON program was used in electric field gradient calculations and the vibrational averaging procedure.

As implemented in MOLPRO,[28,31] analytical and numerical gradients have been used for the MP2 and CCSD(T) geometry optimizations, respectively. As concerns numerical gradients, the step-sizes used were 0.0005 Å for bond distances and 0.1 degrees for bond angles. A convergency criterion stronger than the default one has been employed: we have constrained the maximum component of the gradient and the maximum component of the step to be less than 1.0×10^{-5} au.

As far as the dipole moment computations are concerned, this property has been evaluated as a first derivative of the total energy with respect to a homogeneous electric field at zero field strength. More precisely, the results have been obtained from computations in which finite perturbations with electric field strengths of ±0.0001 au have been applied and thus the dipole moment has been calculated from central-differences numerical differentiation of the energy.

At the MCSCF level of theory the electric field gradients have been evaluated as an expectation value of the corresponding one-electron operator by using the MOLPRO program. Because of the nonvariational nature of the MP2 and CCSD models, the calculations of expectation values are not generally available with the MOLPRO program; thus, the DALTON integral-direct implementation of first-order one-electron properties in the MP2 and CCSD models has been employed.

To evaluate the zero-point vibrational corrections to the molecular structure, dipole moment, and quadrupole coupling constants, a vibrational averaging procedure has been performed. In DALTON, a formalism for the calculation of these corrections to molecular properties has been recently implemented.[32,33] In this approach the contribution to the vibrational corrections from anharmonicity of the potential is included by performing a perturbation expansion of the vibrational wave function around an effective geometry r_{eff}, which can be considered a good approximation to the vibrationally averaged molecular geometry, i.e., the r_0 structure.[32,33] Because the vibrational averaging procedure is computationally very expensive and implemented in DALTON only at the SCF and MCSCF levels of theory, these calculations have been performed by employing the restricted active space self-consistent field (RASSCF) method in conjuction with basis sets of double and triple-ζ quality. More precisely, 17 orbitals and 24 electrons have been taken as active, but only single and double excitations have been considered. Thus, only the 1s core orbitals of F, C, and N atoms have been taken as inactive. As concerns the bases, the cc-pVTZ, aug-cc-pV*n*Z (n = D, T) and cc-pwCV*n*Z (n = D, T) sets have been chosen because they are relatively small but property-oriented: the cc-pVTZ and cc-pwCV*n*Z sets for molecular structure determinations, the aug-cc-pV*n*Z for dipole moment computations and the cc-pwCV*n*Z (n = D, T) bases for electric field gradient evaluations.

3. Equilibrium Properties

3.1. Equilibrium Structure. The equilibrium geometries of difluoromethanimine computed at the CCSD(T) and MP2 levels of theory using different basis sets are summarized in Table 1 following the labeling of the atoms reported in Figure 1.

First of all, we can notice that, as expected, at the CCSD(T) levels, improvements in the basis sets shorten the bond distances. Because a hierarchical sequence of bases has been employed, the asymptotic convergence of the molecular properties mimics that of the energy (see for example, Feller,[36] Peterson and Dunning,[34] and Halkier et al.[35]), and thus it is possible to extrapolate the molecular parameters to the valence correlation limit using the CCSD(T)/cc-pV*n*Z optimized geometries. This has been carried out by combining the $a + bX^{-3}$ extrapolation formula for the correlation contributions[36,37] and the exponential form $A + B \exp(-CX)$ for extrapolation at the SCF level;[34,38] where in both formulas $X = 3$ for the cc-pVTZ basis, $X = 4$ for cc-pVQZ, and so on. The extrapolated CCSD(T)/cc-pV∞Z geometry yielded by this procedure is reported in Table 1. Comparing the CCSD(T)/cc-pV5Z and CCSD(T)/cc-pV∞Z shows that the valence correlation limit is nearly reached at the CCSD(T)/cc-pV5Z level; in fact, only discrepancies lower than 0.001 Å for bonds and 0.1° for angles have been found between the two structures.

TABLE 1: Equilibrium Geometries of F_2CNH Computed at Different Levels of Theory[a] Employing Different Basis Sets, Compared with Previous ab Initio Calculations and Experiment (Best Estimates of the Equilibrium Structure and Extrapolated Geometry to Valence Correlation Limit Also Reported)

	CF_{cis} (Å)	CF_{trans} (Å)	CN (Å)	NH (Å)	$\angle NCF_{cis}$ (deg)	$\angle NCF_{trans}$ (deg)	$\angle CNH$ (deg)	ref
MP2/6-31G(d)	1.3368	1.3198	1.2504	1.0192	128.30	123.26	110.81	7
MP2/6-31G(d,p)	1.3362	1.3199	1.2504	1.0146	128.28	123.26	110.23	7
MP2/6-311G**	1.326	1.310	1.246	1.016	128.3	123.3	110.3	9
CCSD(T)/cc-pVTZ	1.3236	1.3089	1.2468	1.0154	128.14	123.26	110.02	8
CCSD(T)/cc-pVQZ	1.3219	1.3069	1.2433	1.0140	128.17	123.30	110.48	this work
CCSD(T)/cc-pV5Z	1.3217	1.3067	1.2426	1.0140	128.19	123.31	110.62	this work
CCSD(T)/cc-pwCVTZ	1.3225	1.3078	1.2448	1.0148	128.14	123.27	110.07	this work
aCCSD(T)/cc-pwCVTZ	1.3208	1.3062	1.2425	1.0136	128.10	123.29	110.27	this work
CCSD(T)/cc-pwCVQZ	1.3217	1.3067	1.2429	1.0141	128.17	123.31	110.49	this work
aCCSD(T)/cc-pwCVQZ	1.3197	1.3048	1.2402	1.0128	128.12	123.33	110.71	this work
MP2/cc-pwCV5Z	1.3218	1.3061	1.2416	1.0124	128.39	123.26	110.72	this work
aMP2/cc-pwCV5Z	1.3197	1.3041	1.2385	1.0111	128.34	123.29	110.93	this work
CCSD(T)/cc-pV∞Z[b]	1.3217	1.3067	1.2419	1.0140	128.21	123.33	110.73	this work
best estimate 1[c]	1.3197(19)	1.3047(14)	1.2392(25)	1.0127(7)	128.16(6)	123.35(5)	110.95(14)	this work
best estimate 2[d]	1.3196(19)	1.3046(14)	1.2388(25)	1.0127(7)	128.16(6)	123.35(5)	110.94(14)	this work
scaled r_e[e]	1.3210	1.3068	1.2412	1.0197	128.15	123.12	110.72	8
empirical r_e[f]	1.3200	1.3070	1.2421	1.0126	128.04	123.12	110.96	8
empirical r_e − II[g]	1.3212(49)	1.3039(46)	1.2398(7)	1.0116(11)	128.08(44)	123.42(46)	111.14(17)	7

[a] aCCSD(T) and aMP2 mean CCSD(T) and MP2 calculations correlating all electrons, respectively. [b] Evaluated from the CCSD(T)/cc-pV*n*Z geometries using X^{-3} extrapolation technique; see text. [c] Best estimated equilibrium geometry employing eq 1; see text. The core correlation corrections have been evaluated at the CCSD(T)/cc-pwCVQZ level. [d] Best estimated equilibrium geometry employing eq 1; see text. The core correlation corrections have been evaluated at the MP2/cc-pwCV5Z level. [e] Shifted equilibrium geometry obtained from an empirical refinement of the anharmonic force field. [f] Equilibrium geometry obtained from a least-squares fit involving experimental ground-state rotational constants and theoretical vibration−rotation interaction constants (quadratic force constants at the CCSD(T)/cc-pVTZ level and cubic and quartic force constants at the MP2/cc-pVTZ level). [g] Equilibrium geometry obtained from a least-squares fit involving experimental ground-state rotational constants and theoretical vibration−rotation interaction constants (from an anharmonic force field at the MP2/6-31G(d,p) level plus unique scaling factor of 0.95)

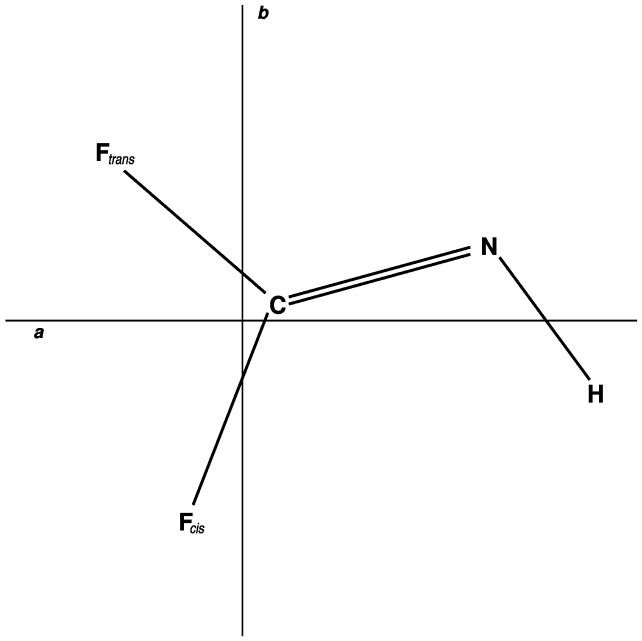

Figure 1. Molecular geometry of $F_2C{=}NH$ with principal inertial axes. The *c* axis (not shown) is perpendicular to the *ab* symmetry plane.

To recover the core-valence corrections, geometry optimizations both correlating only valence and all electrons have been performed. As expected, by comparing frozen core and all electrons calculations, we notice a shortening of all bond lengths when all electrons are correlated. More precisely, shortenings of about 0.001−0.003 Å have been found. The $\angle NCF_{cis}$ and $\angle NCF_{trans}$ bond angles present negligible changes: ∼0.05 and ∼0.02°, respectively. Larger variations have been found for the ∠CNH angle, i.e., by about 0.2°; anyway, they are less than 0.5%.

By using the above-mentioned computations, to provide our best estimate of the equilibrium structure, we have recovered the core correlation effects affecting the CCSD(T)/cc-pV∞Z structure by assuming the additivity of these effects. Thus, as suggested by Martin and Taylor,[39] we have employed the following expression to obtain a best estimate of the equilibrium geometry:

$$r_e \simeq r(\text{cc-pV}\infty\text{Z},valence) + r(\text{wCV}n\text{Z},all) - r(\text{wCV}n\text{Z},valence) \qquad (n = \text{Q}, 5) \quad (1)$$

where *valence* and *all* mean computations correlating only valence and all electrons, respectively. The resulting structures, reported in Table 1 are denoted "best estimate 1" and "best estimate 2" according to whether the CCSD(T)/cc-pwCVQZ or the MP2/cc-pwCV5Z geometries have been used, respectively. First of all, it is apparent that the two best estimate structures perfectly agree. This seems to point out that the MP2 method is able to reasonably recover the core correlation corrections in geometry optimizations.

Before comparing our best estimates to experiment, it is important to evaluate the errors affecting them. From the basis-set investigations performed, we can deduce an uncertainty of ∼0.0003 Å for bond distances and ∼0.03−0.12° for angles (the large uncertainty is related to ∠CNH). The errors arising from the truncation of the model employed have been deduced from the changes in the series HF, CCSD, and CCSD(T): ∼0.0007−0.002 Å for bonds and ∼0.03−0.08° for angles. Thus, by combining the errors, we have obtained the following uncertainties affecting our best estimate structures: ∼0.001−0.002 Å for distances and ∼0.05−0.1° for angles.

As far as experiment is concerned, essentially due to the size of the molecule, only empirical determinations of the equilibrium structure are available. Going into detail, one of the authors[8] determined the equilibrium geometry in two different ways: the first (reported in Table 1 as "scaled r_e") from the empirical refinement of the anharmonic force field evaluated at the CCSD(T)-MP2/cc-pVTZ level (the CCSD(T) model for the harmonic part, the MP2 for the anharmonic one), the second (reported in

TABLE 2: Equilibrium Dipole Moment Evaluated at the CCSD(T)[a] Level Employing Different Basis Sets[b] and the Best Estimate and the Extrapolated Dipole Moment to the Valence Correlation Limit [All Calculations Performed at the "Best Estimate 1" Geometry; Values in Debye (D)]

	CCSD(T)/ aVTZ	CCSD(T)/ aVQZ	CCSD(T)/ aV5Z	CCSD(T)/ awCVTZ	CCSD(T)/ awCVQZ	aCCSD(T)/ awCVTZ	aCCSD(T)/ awCVQZ
μ_a	0.391	0.402	0.406	0.394	0.403	0.404	0.416
μ_b	−1.381	−1.382	−1.383	−1.378	−1.380	−1.382	−1.384

	CCSD(T)/[c] aug-cc-pV∞Z	aCCSD(T)/[c] aug-cc-pwCV∞Z	best estimate 1[d]	best estimate 2[e]
μ_a	0.410	0.428	0.427(10)	0.422(10)
μ_b	−1.384	−1.385	−1.381(4)	−1.384(4)

[a] aCCSD(T) means CCSD(T) calculations correlating all electrons. [b] aV*n*Z (n = T, Q, 5) means aug-cc-pV*n*Z (n = T, Q, 5); awCV*n*Z (n = T, Q) means aug-cc-pwCVnZ (n = T, Q). [c] Extrapolated dipole moment to the valence correlation limit: see text. [d] Best estimate of the equilibrium dipole moment derived by the exprapolated aCCSD(T)/aug-cc-pwCV∞Z value: see text. [e] Best estimate of the equilibrium dipole moment derived by the exprapolated CCSD(T)/aug-cc-pV∞Z value: see text.

Table 1 as "empirical r_e") by using a least-squares fit involving experimental vibrational ground-state rotational constants and theoretical vibrational corrections. Another empirical equilibrium structure was provided by Groner et al.[7] (reported in Table 1 as "empirical r_e-II"), who used a least-squares fit involving experimental ground-state rotational constants and theoretical vibrational corrections derived from a scaled force field (unique scale factor equal to 0.95) evaluated at the MP2/6-31G(d,p) level.

By comparing our estimates of the equilibrium geometry to the empirical structures, we notice a fairly good agreement: in general, they agree within the uncertainties. More precisely, discrepancies of the order of the accuracy of our best estimates have been found: ∼0.002 Å (0.003 Å in the worst cases) for bond distances and ∼0.1° (0.2° in the worst case). Only the NH bond length of the "scaled r_e" is clearly too long (by about 0.007 Å).

As concerns the comparison with the previous theoretical determinations, a noticeable improvement both in the method and in the basis set description has been carried out. This is clear from the results reported and compared in Table 1.

3.2. Dipole Moment. The dipole moment evaluations have been carried out at the best estimate equilibrium structure ("best estimate 1" reported in Table 1) by employing different basis sets including both diffuse, for an accurate description of the outer valence regions, and tight functions, for taking into account core correlation effects. The frozen core computations have been performed with both the aug-cc-pV*n*Z and aug-cc-pwCV*n*Z basis sets, whereas all electron calculations have been carried out only by employing the aug-cc-pwCV*n*Z basis. The values of the μ_a and μ_b components of the equilibrium dipole moment, along the *a* and *b* inertial axes, respectively, obtained at the CCSD(T) level with various basis sets are reported in Table 2.

First of all, we notice that employing both the aug-cc-pV*n*Z and aug-cc-pwCV*n*Z sets both μ_a and μ_b increase in absolute value by expanding the basis. But, it is worth noting that the absolute value of both components of the dipole moment at the SCF level decreases by enlarging the basis, while the correlation contribution increases. Because the correlation contribution $\Delta\mu^{CORR}$ varies more quickly than the SCF contribution μ^{SCF}, the total behavior is explained.

Because we have used hierarchical sequences of bases and both μ^{SCF} and $\Delta\mu^{CORR}$ present a monotonic trend, it is possible to extrapolate the dipole moment to the valence correlation limit. As shown by Halkier et al.,[36] the asymptotic convergence of the correlation contribution to the dipole moment is of the form

$$\Delta\mu_X^{CORR} = \Delta\mu_\infty^{CORR} + aX^{-3} \qquad (2)$$

where $X = 3$ for triple-ζ basis, $X = 4$ for quadruple-ζ and so on. Using eq 2, we have evaluated the infinite basis set limit of the correlation contribution to μ_e both for the aug-cc-pV*n*Z (frozen core) and aug-cc-pwCV*n*Z (all electrons) series. As for geometric parameters, the convergence of the dipole moment at the SCF level is expected to follow the exponential form $A + B\exp(-CX)$ of the SCF energy.[34] Thus, using this exponential law we have extrapolated the infinite basis limit of μ at the SCF level, μ_∞^{SCF}, for both the series. By adding the correlation contribution $\Delta\mu_\infty^{CORR}$ to μ_∞^{SCF}, we have obtained the extrapolated values [(a)CCSD(T)/aug-cc-p(wC)V∞Z] reported in Table 2. By comparing them to each other, we can notice that, as concerns μ_b, they perfectly agree, whereas the μ_a components differ by about 4%. This difference is essentially due to the core-valence corrections.

The extent of the core correlation effects for this property has been estimated by comparing the values obtained from frozen core and all electrons CCSD(T)/aug-cc-pwCVQZ calculations. It is interesting to note that though they seem to be small but not negligible, i.e., ∼3%, for μ_a, they are completely negligible, i.e., less that 0.1%, for μ_b. Anyway, it is noteworthy that by using the aug-cc-pwCV*n*Z series of basis sets, convergence seems to be reached at the CCSD(T)/aug-cc-pwCVQZ level, and therefore with a smaller basis with respect to the aug-cc-pV5Z.

To provide a best estimate of the equilibrium dipole moment, we have followed two procedures. First, an estimate of the correction due to the connected quadruples[40] has been added to the extrapolated aCCSD(T)/aug-cc-pwCV∞Z value. This correction seems to be negligible (less than 0.001 D) for μ_a, whereas it is about 0.005 D for the μ_b component. This first best estimate of the dipole moment has been denoted as "best estimate 1" and is reported in Table 2. Second, the core-valence corrections previously estimated and the estimate of the connected quadruples correction have been added to the extrapolated CCSD(T)/aug-cc-pV∞Z value. This value, denoted as "best estimate 2", is also given in Table 2. Finally, evaluating the errors due to both the basis-set truncation and the *N*-electron model used, the apparent errors have been deduced. By comparing the two best estimates, we can notice that they agree very well, i.e., within the stated uncertainties.

3.3. Quadrupole Coupling Tensors. The elements of the inertial nuclear quadrupole coupling tensor can be evaluated from field gradient q_{ij} calculations at the quadrupolar nucleus:

$$\chi_{ij} = eQq_{ij} \qquad i, j = a, b, c \qquad (3)$$

where χ_{ij} is the ij element of the nuclear quadrupole coupling

TABLE 3: Inertial[a] and Principal Quadrupole[b] Tensors for ^{14}N and D in F_2CNH Computed at Different Levels of Theory[c] Employing Different Basis Sets[d] (All Calculations Performed at the "Best Estimate 1" Geometry)

	MCSCF/ wCVTZ	MCSCF/ wCVQZ	MCSCF/ wCV5Z	MP2/ wCVTZ	MP2/ wCVQZ	CCSD/ wCVTZ	CCSD/ wCVQZ	exp[e]
				^{14}N[f]				
χ_{aa} (MHz)	1.141	1.114	1.053	1.259	1.219	1.217	1.180	1.029(20)
χ_{bb} (MHz)	−2.666	−2.680	−2.567	−2.519	−2.553	−2.771	−2.813	−2.560(17)
χ_{ab} (MHz)	−1.729	−1.729	−1.889	−1.546	−1.519	−1.644	−1.626	
χ_{zz} (MHz)	−3.334	−3.350	−3.373	−3.071	−3.089	−3.362	−3.391	
χ_{xx} (MHz)	1.809	1.784	1.859	1.811	1.755	1.807	1.759	
$\chi_{yy} = \chi_{cc}$ (MHz)	1.525	1.566	1.514	1.260	1.334	1.555	1.632	1.531(22)
θ_{zb} (deg)	21.12	21.18	23.11	19.65	19.43	19.76	19.57	
				D[g]				
χ_{aa} (MHz)	0.086	0.083	0.081	0.086	0.082	0.085	0.081	
χ_{bb} (MHz)	0.048	0.046	0.047	0.049	0.046	0.049	0.047	
χ_{ab} (MHz)	−0.201	−0.193	−0.190	−0.201	−0.192	−0.201	−0.192	
$\chi_{z'z'}$ (MHz)	0.269	0.259	0.255	0.269	0.257	0.269	0.256	
$\chi_{x'x'}$ (MHz)	−0.135	−0.130	−0.127	−0.135	−0.128	−0.135	−0.128	
$\chi_{y'y'} = \chi_{cc}$ (MHz)	−0.134	−0.129	−0.128	−0.134	−0.128	−0.134	−0.128	
$\theta_{z'a}$ (deg)	42.30	42.27	42.61	42.30	42.31	42.44	42.46	

[a] *a*, *b*, and *c* denote the principal inertial axes (see text). [b] *x*, *y*, and *z* denote the principal nitrogen quadrupole axes; *x*′, *y*′, and *z*′ the principal deuterium quadrupole axes (see text). [c] MCSCF: 20 electrons in 15 orbitals as active space (see text). MP2 and CCSD: all electrons as active. [d] wCV*n*Z (*n* = T, Q, 5) means cc-pwCV*n*Z (*n* = T, Q, 5). [e] Experimental data for the fundamental isotopomer.[3] Experimental data for the isotopic species containing ^{13}C ($F_2{}^{13}C^{14}NH$):[6] $\chi_{aa}(^{14}N) = 1.017(14)$ MHz, $\chi_{bb}(^{14}N) = -2.532(12)$ MHz, $\chi_{cc}(^{14}N) = 1.515(21)$ MHz. [f] Evaluated for the fundamental isotopic species: $F_2C^{14}NH$. [g] Evaluated for the deuterated isotopic species: $F_2C^{14}ND$.

tensor, *e* is the electron charge, *Q* is the nuclear electric quadrupole moment of the nucleus considered, and finally, *a*, *b* and *c* are the inertial axes (where the *c* axis is perpendicular to the molecular plane *ab*; see Figure 1).

Because difluoromethanimine is a planar molecule, for each quadrupolar nucleus the inertial nuclear quadrupole tensor has only one off-diagonal nonzero element, which is χ_{ab}:

$$\chi^{I}(^{14}\text{N or D}) = \begin{pmatrix} \chi_{aa} & \chi_{ab} & 0 \\ \chi_{ab} & \chi_{bb} & 0 \\ 0 & 0 & \chi_{cc} \end{pmatrix} \quad (4)$$

More precisely, the values of q_{ij} have been converted into the values of splitting constants by using the following expression:

$$\chi_{ij}\,(\text{MHz}) = 234.9647 \times Q\,(\text{barn}) \times q_{ij}\,(\text{au}) \quad (5)$$

where we have used $Q(^{14}N) = 0.02044$ barn and $Q(D) = 0.00286$ barn, both from Pyykkö.[41] All these computations have been performed at the best estimate equilibrium structure ("best estimate 1"); the results obtained are listed in Table 3.

The inertial nuclear quadrupole coupling tensors have been diagonalized to yield the principal nuclear quadrupole coupling tensors and the rotation angles θ_{zb} (angle between the *z* and *b* axes) for the nitrogen atom and $\theta_{z'a}$ (between the *z*′ and *a* axes) for the deuterium atom; where *x*, *y*, and *z* are the principal nitrogen quadrupole axes and *x*′, *y*′, and *z*′ the principal deuterium quadrupole axes, arranged to have the *y* and *y*′ axes coincident with the *c* one. The results are collected in Table 3.

First of all, from this table it is observed that differences between the various methods are of the order of ∼5−20%, where, in general, the largest deviations are exhibited by the nitrogen constants. However, it should be noted that these large deviations essentially come from the smallness of the parameters; indeed, only variations in the range 0.005−0.3 MHz have been found. In particular, for the D nucleus the largest discrepancies have been found to be in the range 0.003−0.011 MHz; this is due to the particular smallness of these coupling constants. For ^{14}N the largest differences vary from 0.1 to 0.37 MHz.

As concerns the convergence with basis sets, we only have the results for a hierarchical sequence of bases to compare at the MCSCF level. This method does not present a clear trend for either the nitrogen or deuterium atoms, and there is only a little change of all parameters moving from one basis to another. In regard to the MP2 and CCSD methods, from the cc-pwCVTZ to cc-pwCVQZ basis sets they present the same behavior evidenced at the MCSCF level. These results suggest that the numerical instability of all these methods prevails over the size of the basis as relatively small constants are considered. The results reported by one of the authors in ref 42 seem to draw the same conclusions. On the whole, from our past experience for both diatomic and polyatomic molecules,[42,43−47] the accuracy of these computations is expected to be of the order of 3−5%.

In Table 3 a few available experimental data are also reported, but because they are vibrational ground-state data and not equilibrium ones, a detailed discussion about the comparison between experiment and theory will be given in the "vibrationally averaged properties" section. Nevertheless, because from our past experience[42,45,46] the vibrational corrections to this property are in general negligible or at least very small, we can notice that the calculated values at all the levels of theory considered here seem to be slightly overestimated.

4. Vibrationally Averaged Properties

4.1. Effective Structure. As previously mentioned, in the Computational Details, the effective geometry r_{eff} can be considered a good approximation to the vibrationally averaged molecular geometry r_0 structure. r_e and r_{eff} obtained at the RASSCF/cc-pVTZ, RASSCF/cc-pwCV*n*Z (*n* = D, T) and RASSCF/aug-cc-pVTZ levels are reported in Table 4.

First of all, from this table one sees that at all levels of theory the effective distances are 0.001−0.006 Å longer than the equilibrium ones; as concerns bond angles, we notice increases in the range of 0.02−0.4 degrees moving from the equilibrium to the effective geometry. Going into detail, the smallest variation, ∼0.001 Å, is on the N−H bond, whereas elongations by about 0.005−0.006 Å have been found for $C-F_{cis}$ and $C-F_{trans}$ bond lengths and by about 0.003 Å for C═N. As concerns bond angles, the smallest variations, ∼0.02−0.04°, are presented by

TABLE 4: Equilibrium and Effective Geometries of F_2CNH Computed at the RASSCF Level Employing Different Basis Sets[a] Compared to the Experimental r_0 (Best Estimate of the Zero-Point Averaged Structure Also Reported)

	CF_{cis} (Å)	CF_{trans} (Å)	CN (Å)	NH (Å)	∠NCF_{cis} (deg)	∠NCF_{trans} (deg)	∠CNH (deg)	ref
RASSCF/VTZ-r_e	1.3162	1.3034	1.2470	1.0188	127.86	123.26	109.49	this work
RASSCF/VTZ-r_{eff}	1.3218	1.3088	1.2500	1.0203	127.96	123.30	109.86	this work
RASSCF/aVTZ-r_e	1.3162	1.3033	1.2472	1.0187	127.89	123.23	109.66	this work
RASSCF/aVTZ-r_{eff}	1.3218	1.3087	1.2503	1.0201	127.97	123.26	109.99	this work
RASSCF/wCVDZ-r_e	1.3253	1.3117	1.2501	1.0269	127.90	123.29	108.75	this work
RASSCF/wCVDZ-r_{eff}	1.3310	1.3173	1.2532	1.0286	128.00	123.34	109.06	this work
RASSCF/wCVTZ-r_e	1.3161	1.3032	1.2463	1.0185	127.85	123.28	109.52	this work
RASSCF/wCVTZ-r_{eff}	1.3217	1.3086	1.2494	1.0199	127.97	123.30	109.89	this work
estimated r_0[b]	1.325(4)	1.310(3)	1.243(8)	1.014(6)	128.3(3)	123.4(2)	111.3(14)	this work
experimental r_0[c]	1.3227(26)	1.3147(26)	1.2397(49)	1.0200(32)	128.78(18)	123.13(14)	110.23(22)	6
experimental r_0[d]	1.318(97)	1.316(92)	1.244(14)	1.021(19)	128.9(87)	122.7(91)	109.9(36)	7

[a] VTZ, aVTZ and wCV*n*Z (n = D, T) mean cc-pVTZ, aug-cc-pVTZ, and cc-pwCV*n*Z (n = D, T) basis sets, respectively. [b] Obtained by adding the vibrational corrections to the "best estimate 1" structure; see text. [c] In the fit the difference between CF_{cis} and CF_{trans} has been fixed at the X-ray value.[5] [d] Only rotational constants A and B were used.[7]

TABLE 5: Equilibrium and Vibrationally Averaged Dipole Moment Evaluated at the RASSCF/aug-cc-pV*n*Z (n = D, T) Level and Best Estimate of the Vibrational Ground State Dipole Moment and Experimental Values [Values in Debye (D)]

	RASSCF/aug-cc-pVDZ			RASSCF/aug-cc-pVTZ				
	equilibrium geometry	effective geometry	vibrationally averaged	equilibrium geometry	effective geometry	vibrationally averaged	estimated[a] μ_0	exp[b,c,d] μ_0
μ_a	0.379	0.424	0.426	0.386	0.431	0.474	0.51(4)	0.415(1) 0.235(1)
μ_b	−1.396	−1.384	−1.358	−1.413	−1.401	−1.313	−1.28(3)	1.330(1) 1.438(2)

[a] Best estimate of the zero-point averaged dipole moment: see text. [b] Groner et al.[3] from Stark spectroscopy (only the absolute value of the dipole moment can be evaluated): upper line. [c] Groner et al.[6] from Stark spectroscopy (only the absolute value of the dipole moment can be evaluated): lower line. [d] Möller et al.[2] from Stark spectroscopy (only the absolute value can be evaluated): μ_b = 1.800(73) D.

∠NCF_{trans}, whereas the largest, ∼0.31−0.38°, by ∠CNH; for ∠NCF_{cis} the increases are of the order of 0.1°.

To determine a more accurate r_0 structure, we have assumed the additivity of these corrections. More precisely, we have added the differences between r_e and r_{eff} evaluated at the RASSCF/cc-pwCVTZ level to our best estimate ("best estimate 1" reported in Table 1); the geometry obtained in such a way, denoted as "estimated r_0", is reported in Table 4. The errors affecting this structure have been estimated both from the differences between the parameters of the best estimate geometry and those at the RASSCF/cc-pwCVTZ level and from the uncertainties affecting the best estimate itself.

The "estimated r_0" can be directly compared to the experimental r_0 geometry, also given in Table 4. Two different determinations of the experimental r_0 are available in the literature, both of them by Groner and co-workers.[6,7] The first evaluation[6] was carried out in 1996, and the assumption that the difference between C−F_{cis} and C−F_{trans} distances is fixed at the X-ray value was made; the second one[7] was performed in 2001 without any approximation but only employing A and B rotational constants. For both determinations, the isotopic data came from four species: $F_2C^{14}NH$, $F_2{}^{13}C^{14}NH$, $F_2C^{15}NH$, and $F_2C^{15}ND$.

By examining our estimate and experiment, although we have made use of an addidive approximation, we can notice that they compare quite well: in general, they agree within the errors. The largest deviation is presented by the ∠CNH bond angle, for which the theoretical value is, however, affected by a large uncertainty due to the difference between the RASSCF/cc-pwCVTZ and best estimate results.

4.2. Dipole Moment. The vibrational averaging of the dipole moment has been carried out at the RASSCF/aug-cc-pV*n*Z (n = D, T) level; the results obtained are summarized in Table 5.

By comparing μ_e and μ_{eff} obtained at the above-mentioned levels, first of all, one sees that for both the μ_a and μ_b components the zero-point vibrational corrections are not negligible. Going into detail, the vibrational corrections increase μ_a but decrease μ_b. In Table 5 not only the equilibrium and vibrationally averaged values but also those evaluated at the r_{eff} geometry are reported; this allows us to determine the extent of the vibrational corrections due to the shift in geometry and that due to the property derivatives. It is apparent that for μ_a both the shift in geometry and property derivatives contribute to the zero-point corrections, whereas for μ_b only the property derivatives contribute. This is also confirmed by evaluating μ_a and μ_b at the "estimated r_0" geometry at the (all electrons) CCSD(T)/aug-cc-pwCVQZ level: μ_a = 0.445 D and μ_b = −1.386 D. By comparing these results with those obtained at the "best estimate 1" structure at the same level of theory, we notice that μ_a increases by ∼7%, whereas μ_b is practically unchanged.

Finally by comparing μ_e and μ_{eff} at the RASSCF/aug-cc-pVTZ level, an estimate of the zero-point corrections can be deduced. By assuming the additivity of this correction to our best estimate equilibrium dipole moment (a mean value of the "best estimate 1" and "best estimate 2" μ_e has been considered), a best estimate of the vibrational ground-state dipole moment μ_0 can be obtained. Before comparing it to experiment, an estimation of the uncertainties affecting this evaluation has been carried out. As for the "estimated r_0", for each component the error has been estimated both from the difference between the value of the best estimate and the μ_e at the RASSCF/aug-cc-pVTZ level and from the uncertainties affecting the best estimate equilibrium dipole moment itself.

In regard to experiment, three different determinations of μ_0 are available in the literature, all from Stark spectroscopy, and they are reported in Table 5. Two of them were carried out by

TABLE 6: RASSCF/cc-pwCVnZ (n = D, T) Inertial[a] and Principal[b] Quadrupole Coupling Tensors of the Main (^{14}N) and Deuterated (D) Species Evaluated at the Equilibrium and Effective Geometries and Vibrationally Averaged Tensors (Estimates of the Zero-Point Corrected Quadrupole Coupling Constants and Experimental Data Also Given; All Values in MHz)

	RASSCF/cc-pwCVDZ			RASSCF/cc-pwCVTZ				
	equilibrium geometry	effective geometry	vibrationally averaged	equilibrium geometry	effective geometry	vibrationally averaged	estimated[c] χ_0	exp[d]
				^{14}N				
χ_{aa}	1.317	1.348	1.290	1.136	1.174	1.114	1.031(52)	1.029(20)
χ_{bb}	−2.618	−2.655	−2.601	−2.698	−2.740	−2.672	−2.541(76)	−2.560(17)
χ_{ab}	−1.738	−1.716	−1.703	−1.741	−1.715	−1.715	−1.863(75)	
χ_{zz}	−3.276	−3.290	−3.241	−3.370	−3.385	−3.333	−3.336(100)	
χ_{xx}	1.974	1.983	1.931	1.809	1.819	1.775	1.825(76)	
χ_{yy} (=χ_{cc})	1.301	1.307	1.310	1.562	1.566	1.558	1.510(60)	1.531(22)
				D				
χ_{aa}	0.084	0.086	0.088	0.086	0.088	0.088		
χ_{bb}	0.044	0.045	0.036	0.044	0.041	0.035		
χ_{ab}	−0.189	−0.187	−0.179	−0.193	−0.191	−0.183		
$\chi_{z'z'}$	0.255	0.252	0.239	0.260	0.257	0.246		
$\chi_{x'x'}$	−0.126	−0.125	−0.119	−0.130	−0.128	−0.123		
$\chi_{y'y'}$ (=χ_{cc})	−0.129	−0.127	−0.120	−0.130	−0.129	−0.123		

[a] a, b, and c denote the principal inertial axes (see text). [b] x, y, and z denote the principal nitrogen quadrupole axes; x', y', and z' the principal deuterium quadrupole axes (see text). [c] Estimated vibrational ground-state nuclear quadrupole coupling constants: see text. [d] Groner et al.[3]

Groner and co-workers,[3,6] who evaluated both μ_a and μ_b, whereas Möller et al.[2] determined only the μ_b component. From Table 5, one sees they are completely in disagreement with one another. In particular, the two evaluations of the μ_a and μ_b components obtained by Groner et al., even if they have the same accuracy, differ by ∼40% and ∼10%, respectively. Because the experimental accuracy of the measurements is not able to discriminate which is the most reliable determination, we can do it on the basis of the highly accurate ab initio calculations performed. By comparing both the equilibrium and vibrational corrected best estimates to experiment, we can conclude that the determination carried out by Groner et al. in 1988 (μ_a = 0.415(1) D and μ_b = 1.330(1) D) seems to be the most reliable and that the theoretical vibrational corrections seem to be slightly overestimated.

4.3. Quadrupole Coupling Tensors. From our past experience[42,45,46] the vibrational corrections to the nuclear quadrupole coupling constants are negligible or, in the worst cases, of the order of the accuracy of the calculations. Consequently, in general, the theoretical equilibrium values can be directly compared to experiment, which gives vibrational ground-state parameters.

Thus, to confirm this, the extent of the zero-point vibrational corrections for nuclear quadrupole coupling constants has been estimated by performing a vibrational averaging procedure at the RASSCF/cc-pwCVnZ level (n = D, T). The results are collected in Table 6.

From this table, it is clear that the vibrational corrections are almost negligible or at maximum of the order of 2%. This means that computed and experimental values reported in Table 3 can be directly compared. Anyway, we can notice that at the RASSCF/cc-pwCVTZ level, the vibrational corrections decrease all the constants for both ^{14}N and D atoms. By assuming the additivity of these small corrections to those we consider our best calculated values, i.e., those at the MCSCF/cc-pwCV5Z level, we have obtained an estimate of the zero-point corrected quadrupole coupling constants denoted as "estimated χ_0". These values are reported in Table 5 in conjuction with an estimate of the uncertainties affecting them, which were derived from the stated accuracy for such calculations, i.e., 3−5%.

By comparing the "estimated χ_0" to the equilibrium MCSCF/cc-pwCV5Z values (Table 3) and to experiment, we can notice an overall good agreement and that the vibrational corrections seem to justify the overestimation of the theoretical parameters summarized in Table 3.

As for the dipole moment, not only the equilibrium and vibrationally averaged values but also those evaluated at the r_{eff} geometry are reported in Table 6; here we can notice that there is not a clear trend: in fact, in most cases the contributions from the shift in geometry and those from the property derivatives are in opposite directions. Finally, it is noteworthy that the vibrational averaged values of χ_{ac} and χ_{bc} both for nitrogen and deuterium atoms still remain equal to zero; this means that the vibrations do not involve a loss of planarity of the molecule.

4.4. Temperature Effect. Because by default (i.e., if the temperature is not specified in the DALTON input) the vibrational averaging procedure is performed at the absolute temperature T = 0 K whereas, on the other hand, the experiments are usually carried out at room temperature, the effect of the temperature on the dipole and quadrupole moments and on the nuclear quadrupole coupling constants has been investigated.

Thus, to evaluate how the temperature T affects the vibrationally averaged properties, the vibrational averaging procedure at the RASSCF/cc-pwCVTZ and RASSCF/aug-cc-pVTZ levels has been performed at four different values of temperature: 0, 100, 200, and 300 K. The results obtained are summarized in Table 7.

From this table it is clear that by increasing the temperature the variations of the vibrationally averaged values are negligible: the dipole and quadrupole moments and the quadrupole coupling constants vary less than 0.5−1%. Therefore, we can conclude that for this molecule the vibrational effects are independent of the temperature. This could be essentially explained by the fact that there are no fundamental vibrational modes at very low frequency.

Finally, following Toyama et al.,[48] the effect of rotation on the molecular dipole moment has been evaluated at 3 different temperatures: 100, 200, and 300 K. To this purpose, the first derivative of this property with respect normal coordinates, harmonic frequencies and other requirements have been computed at the RASSCF/aug-cc-pVTZ level employing the DALTON program. For each temperature, the effect of rotation has been found to be negligible: varying for both components in the range 0.002−0.007 D. This is very likely due to the fact that the molecule does not have any large amplitude motions.

TABLE 7: Temperature Effect on Molecular Vibrationally Averaged Properties Evaluated at the RASSCF/aug-cc-pVTZ and RASSCF/cc-pwCVTZ Levels of Theory for the Fundamental Isotopomer, $F_2C^{14}NH$, and the Deuterated Species, $F_2C^{14}ND$[a]

		$T = 0$ K	$T = 100$ K	$T = 200$ K	$T = 300$ K
		RASSCF/aug-cc-pVTZ			
μ_a	(D)	0.374	0.374	0.374	0.374
μ_b	(D)	−1.313	−1.313	−1.313	−1.312
Θ_{aa}	(a.u.)	0.830	0.830	0.830	0.830
Θ_{bb}	(a.u.)	−1.871	−1.871	−1.871	−1.871
Θ_{ab}	(a.u.)	−3.298	−3.298	−3.298	−3.296
Θ_{cc}	(a.u.)	1.041	1.041	1.041	1.041
		RASSCF/cc-pCVTZ			
$\chi_{aa}(^{14}N)$	(MHz)	1.114	1.114	1.114	1.111
$\chi_{bb}(^{14}N)$	(MHz)	−2.672	−2.672	−2.672	−2.670
$\chi_{ab}(^{14}N)$	(MHz)	−1.715	−1.715	−1.715	−1.715
$\chi_{cc}(^{14}N)$	(MHz)	1.558	1.558	1.558	1.559
$\chi_{aa}(D)$	(MHz)	0.012	0.012	0.012	0.012
$\chi_{bb}(D)$	(MHz)	0.111	0.111	0.111	0.110
$\chi_{ab}(D)$	(MHz)	−0.177	−0.177	−0.177	−0.176
$\chi_{cc}(D)$	(MHz)	−0.123	−0.123	−0.123	−0.122
Θ_{aa}	(a.u.)	0.735	0.735	0.735	0.734
Θ_{bb}	(a.u.)	−1.760	−1.760	−1.760	−1.760
Θ_{ab}	(a.u.)	−3.271	−3.271	−3.270	−3.268
Θ_{cc}	(a.u.)	1.025	1.025	1.025	1.026

[a] Dipole and quadrupole moments have been calculated only for the fundamental Isotopomer.

5. Conclusion

A thorough study of the equilibrium structure and molecular properties of difluoromethanimine has been carried out at a high level of accuracy. In particular, very accurate values of the equilibrium geometry, dipole moment, and nuclear quadrupole tensors are given. Both core correlation and finite basis set effects have been taken into account. A vibrational averaging procedure allowed us to also report the zero-point vibrational corrected values for both structure and molecular properties. Thus, an accurate comparison with available experimental data was feasible.

Although zero-point corrections seem to be negligible or at least very small for nuclear coupling constants, they are quite important in evaluating both the molecular dipole moment and vibrationally averaged r_0 structure. In fact, the vibrational effects give an account of the differences found between experimental r_0 and empirical r_e structures. Furthermore, a very accurate determination of the equilibrium dipole moment in conjuction with the estimation of the vibrational corrections allowed us to discriminate which is the most reliable experimental value.

Acknowledgment. This work has been supported by MIUR (ex-40%), CNR, and the University of Bologna (funds for selected research topics and ex-60% funds). We thank the High Performance Systems Division of the CINECA Supercomputing Center (Interuniversity Consortium) for support in the utilization of computer resources. We gratefully thank Prof. K. A. Peterson for useful discussions and reading the manuscript. C.P. also thanks Prof. G. Cazzoli for supporting this study and for useful discussions.

References and Notes

(1) Bürger, H.; Pawelke, G. *J. Chem. Soc., Chem. Commun.* **1988**, 105.
(2) Möller, K.; Winnewisser, M.; Pawelke, G.; Bürger, H. *J. Mol. Struct.*, **1988**, *190*, 343
(3) Groner, P.; Nanaie, H.; Durig, J. R.; DesMarteau, D. D. *J. Chem. Phys.* **1988**, *89*, 3983.
(4) Bürger, H.; Kuna, R.; Pawelke, G.; Sommer, S.; Thiel, W. *Z. Naturforsch. A* **1992**, *47*, 475.
(5) Pawelke, G.; Dammel, R.; Poll, W. *Z. Naturforsch. B* **1992**, *47*, 351.
(6) Groner, P.; Durig, J. R.; DesMarteau, D. D. *J. Chem. Phys.* **1996**, *105*, 7263.
(7) Groner, P.; Warren, R. D. *J. Mol. Struct.* **2001**, *599*, 323.
(8) Gambi, A. *J. Mol. Spectrosc.* **2002**, *216*, 508.
(9) Pouchan, C.; Gelize-Duvignau, M. *J. Mol. Struct. THEOCHEM* **2002**, *594*, 173.
(10) Hampel, C.; Peterson, K. A.; Werner, H.-J. *Chem. Phys. Lett.* **1992**, *190*, 1.
(11) Raghavachari, K.; Trucks, G. W.; Pople, J. A.; Head-Gordon, M. *Chem. Phys. Lett.* **1989**, *156*, 479.
(12) Deegan, M. J. O.; Knowles, P. J. *Chem. Phys. Lett.* **1994**, *227*, 321.
(13) Møller, C.; Plesset, M. S. *Phys. Rev.* **1934**, *46*, 618.
(14) Dunning, T. H., Jr. *J. Chem. Phys.* **1989**, *90*, 1007.
(15) Peterson, K. A.; Dunning, T. H., Jr. *J. Chem. Phys.* **2002**, *117*, 10548.
(16) Kendall, R. A.; Dunning, T. H., Jr.; Harrison, R. J. *J. Chem. Phys.* **1992**, *96*, 6796.
(17) Woon, D. E.; Dunning, T. H., Jr. *J. Chem. Phys.* **1993**, *98*, 1358.
(18) Woon, D. E.; Dunning, T. H., Jr. *J. Chem. Phys.* **1995**, *103*, 4572.
(19) Demaison, J.; Margulès, L.; Boggs, J. E. *Chem. Phys.* **2000**, *260*, 65.
(20) Margulès, L.; Demaison, J.; Rudolph, H. D. *J. Mol. Struct.* **2001**, *599*, 23.
(21) Vázquez, J.; Demaison, J.; López-González, J. J.; Boggs, J. E.; Rudolph, H. D. *J. Mol. Spectrosc.* **2001**, *207*, 224.
(22) Werner, H.-J.; Knowles, P. J. *J. Chem. Phys.* **1985**, *82*, 5053.
(23) Knowles, P. J.; Werner, H.-J. *Chem. Phys. Lett.* **1985**, *115*, 259.
(24) Halkier, A.; Koch, H.; Christiansen, O.; Jørgensen, P.; Helgaker, T. *J. Chem. Phys.* **1997**, *107*, 849.
(25) Purvis, G. D.; Bartlett, R. J. *J. Chem. Phys.* **1982**, *76*, 1910.
(26) Halkier, A.; Larsen, H.; Olsen, J.; Jørgensen, P.; Gauss, J. *J. Chem. Phys.* **1999**, *110*, 734.
(27) MOLPRO is a package of ab initio programs written by H.-J. Werner and P. J. Knowles, with contributions of R. D. Amos, A. Bernhardsson, P. Celani, D. L. Cooper, M. J. O. Deegan, A. J. Dobbyn, F. Eckert, C. Hampel, G. Hetzer, T. Korona, R. Lindh, A. W. Lloyd, S. J. McNicholas, F. R. Manby, W. Meyer, M. E. Mura, A. Nicklass, P. Palmieri, R. Pitzer, G. Rauhut, M. Schütz, H. Stoll, A. J. Stone, R. Tarroni, and T. Thorsteinsson.
(28) Eckert, F.; Pulay, P.; Werner, H.-J. *J. Comput. Chem.* **1997**, *18*, 1473.
(29) Rauhut, G.; El Azhary, A.; Eckert, F.; Schumann, U.; Werner, H.-J. *Spectrochim. Acta* **1999**, *55*, 651.
(30) "DALTON, a molecular electronic structure program, Release 1.2 2001", written by T. Helgaker, H. J. Aa. Jensen, P. Jørgensen, J. Olsen, K. Ruud, H. Ågren, A. A. Auer, K. L. Bak, V. Bakken, O. Christiansen, S. Coriani, P. Dahle, E. K. Dalskov, T. Enevoldsen, B. Fernandez, C. Hättig, K. Hald, A. Halkier, H. Heiberg, H. Hettema, D. Jonsson, S. Kirpekar, R. Kobayashi, H. Koch, K. V. Mikkelsen, P. Norman, M. J. Packer, T. B. Pedersen, T. A. Ruden, A. Sanchez, T. Saue, S. P. A. Sauer, B. Schimmelpfenning, K. O. Sylverester-Hvid, P. R. Taylor, and O. Vahtra.
(31) El Azhary, A.; Rauhut, G.; Pulay, P.; Werner, H.-J. *J. Chem. Phys.* **1998**, *108*, 5185.
(32) Åstrand, P.-O.; Ruud, K.; Taylor, P. R. *J. Chem. Phys.* **2000**, *112*, 2655.
(33) Ruud, K.; Åstrand, P.-O.; Taylor, P. R. *J. Chem. Phys.* **2000**, *112*, 2668.
(34) Feller, D. *J. Chem. Phys.* **1993**, *98*, 7059.
(35) Peterson, K. A.; Dunning, T. H., Jr. *J. Mol. Struct. THEOCHEM.* **1997**, *400*, 93.
(36) Halkier, A.; Klopper, W.; Helgaker, T.; Jørgensen, P. *J. Chem. Phys.* **1999**, *111*, 4424.
(37) Helgaker, T.; Klopper, W.; Koch, H.; Noga, J. *J. Chem. Phys.* **1997**, *106*, 9639.
(38) Feller, D. *J. Chem. Phys.* **1992**, *96*, 6104.
(39) Martin, J. M. L.; Taylor, P. R. *Chem. Phys. Lett.* **1996**, *248*, 336.
(40) Helgaker, T.; Jørgensen, P.; Olsen, J. *Modern Electronic-Structure Theory*; Wiley: Chichester, U.K., 2000; pp 836−840.
(41) Pyykkö, P. *Z. Naturforsch. A* **1992**, *47*, 189.
(42) Puzzarini, C. *Phys. Chem. Chem. Phys.* **2004**, *6*, 344.
(43) Dore, L.; Puzzarini, C.; Cazzoli, G.; Gambi, A. *J. Mol. Spectrosc.* **2000**, *204*, 262.
(44) Dore, L.; Puzzarini, C.; Cazzoli, G. *Can. J. Phys.* **2001**, *79*, 359.
(45) Puzzarini, C.; Dore, L.; Cazzoli, G. *J. Mol. Spectrosc.* **2003**, *217*, 19.
(46) Puzzarini, C.; Gambi, A.; Cazzoli, G. *J. Mol. Struct.* **2004**, in press.
(47) Puzzarini, C.; Cazzoli, G.; Gambi, A. *J. Chem. Phys.* **2003**, *118*, 2647. Cazzoli, G.; Puzzarini, C.; Gambi, A. *J. Chem. Phys.* **2004**, *120*, 6495.
(48) Toyama, M.; Oka, T.; Morino, Y. *J. Mol. Spectrosc.* **1964**, *13*, 193.